Optimal Longitudinal Controller Design for Rotorcraft under Different Flight Conditions

Zia Ullah
CECOS University, Peshawar, Khyber Pakhtunkhwa, Pakistan
engineerziaullah@yahoo.com

Tanveer Ahmad
CECOS University, Peshawar, Khyber Pakhtunkhwa, Pakistan
tanveer.ahmad89@gmail.com

Muhammad Hilal Khan
CECOS University, Peshawar, Khyber Pakhtunkhwa, Pakistan
hilal@cecos.edu.pk

Abstract

The problem of aerodynamic properties of rotorcraft especially harmonic blade oscillations and rotor vibration transmitted to fuselage are very important with particular reference to rotor. In this paper the longitudinal cyclic pitch, lateral cyclic pitch, main rotor collective pitch angle and tail rotor collective pitch angle are used as control inputs to develop a nonlinear 6 DOF model of a longitudinal rotorcraft. In this research translational/rotational dynamics and rotational kinematic equations of motion are derived for 6 DOF rotorcraft motion about possible equilibrium position. On the basis of these linearized equations, an optimal controller is designed for different flight conditions under different rotor speeds with relevant blade oscillations and rotor vibration effect. Wind tunnel data of an existing rotorcraft is used for simulation purposes. A closed loop feedback controller is designed using MATLAB/ Simulink software. The simulation results obtained by varying control inputs indicate that this approach is well-suited to reduce/eliminate the harmonics blade oscillation and rotor vibration.

Keyword

Control, Stability, Optimal, Linearization, Blade Harmonics.

1. Introduction

The rotor is accountable for three core functions in rotorcrafts; to create a lift force in upward direction opposite to the force of gravity; to create a thrust force in a direction opposite to the drag force for forward flight and source for creating potent actions to control the altitude and position of rotorcraft during hovering condition.

Zioutis et al. [9] studied aerodynamic behaviour of a convoluted helicopter rotor flow field. The research focused on computational investigation about efficiency of developed mathematical models. Using procedures based on Lagrangian type, Vortex Element method, free vertical wake geometry and rotor airloads are calculated. Thanapalan [8] studied modeling and simulation of a single main rotor helicopter, UH-60 Black Hawk helicopter. The simulation study consists of a Generic Rotorcraft Model (GRM) that calculated the forces and moment expressions. The simulation results are compared with the flight test data. The model provided a clear idea for controller development to improve flight handling quality and performances. Houbolt and Brooks [4] worked on the flap-lag-torsion stability of elastic hingeless blades. In their work only linear flap-lag coupling were considered while the nonlinear bending torsion coupling terms were not included. Mil' et al. [6] investigated the complete flap-lag-torsion stability problem. The research showed that nonlinear structural moments caused by flap and lead-lag bending greatly affect the torsion deflection of the hingeless blade. This bending-torsion was detected to be proportional to the product of the flap and lead-lag bending curvatures. Arcidiacono [1] derived some nonlinear equations of motion which explained the nonlinear flap-lag-torsion coupling problem in a complete and detailed way. The research ignored some nonlinear terms in the derivation. David [2] worked on an analytical model for calculating the forces between the rigid bodies i.e. rotor blades and a non-colliding contact. The work described the rigid bodies in motion or static equilibrium where adjacent bodies may touch at multiple points. The equations of forces for bodies in non-colliding contact are being modified to deal with colliding bodies. Similarly an improved method for calculating the forces between systems of rigid bodies in colliding contacts is also presented. Datta [3] investigated accurate and reliable estimate of rotor vibratory loads in steady level flight. The leading source of helicopter vibration is the rotor vibratory loads. According to the author the helicopter has two dangerous states of vibrations in steady level flight, which are low state transition and high speed forward flight. The study describes that at low speed the rotor mechanism i.e. inter linking of blade tip vortices below the rotor disk is well understood but at high speed the mechanism is not clear. The research focuses on high speed flight. The ultimate goal of the research is to understand the mechanism and to accurately model them. To improve the rotor structure the measured lift chord force pitching moment and damper force are taken from the UH60 Flight Test Program. Potsdam et al. [7] calculated the helicopter rotor air loads across a range of flight conditions. For this purpose the authors studied a Computational Fluid Dynamics (CFD) code and rotorcraft Computational Structural Dynamics (CSD). For a UH-60A Blackhawk helicopter, four challenging level flight conditions are computed i.e. low speed with blade-vortex interaction, high speed with advancing blade negative lift, high thrust with dynamic stall, and hover. Results are compared with UH-60A airloads program flight test data. Juho Ilkko et al. [5] worked on a computational model that treated the four blades of a helicopter as rigid body, hinged at their roots. The authors examined the vibrant actions of motion caused by the blade angle controls. Using the Reynolds averaged Navier-Stokes equations, a time-accurate flow solution is presented with the help of an overset grid system consisting of around 20 million cells, hover and fast flight forward case are studied.

Different rotorcraft motions are controlled with the help of variable pitch propellers that undergoes certain elastic deformations by collision with the surrounding air. Desired motions can be achieved by twisting the blades in certain directions or in other words changing the pitch angle of the blades results in a successful change in the angle of attack (α) that depends on the direction of the relative wind. A change in the position of the blade shall change the direction of the thrust force and accordingly the motion of the rotorcraft is controlled. The collision of rotor blades with the surrounding air acts as an action and reaction forces. During hovering and forward flight condition different forces act on a rotor craft as shown in Fig (1).

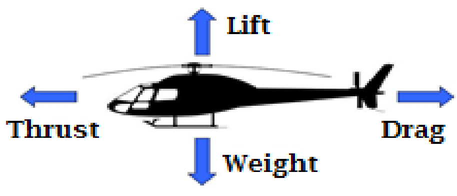

Fig 1: Forces acting on rotorcraft

The thrust force is produced as per Newton's Laws of motion, when a system expels or accelerates mass in one direction, the accelerated mass will cause a force of equal magnitude but opposite direction on that

system. Thrust force has a direct relation with the rpm i.e. an increase in rpm more air is accelerated by the propeller as a result more thrust force is generated. For a rotorcraft system, drag force is referred as a frictional force with a direction opposite to the thrust force. Lift force is a reaction force that is exerted by the air on the airfoil as it moves through the air. It means that when the propeller rotates in the air it exerts a pressure force on the air in downward direction and the air also exerts a force same in magnitude on the propeller but opposite in direction. Lift force increases until it overcomes the weight of the helicopter as a result the helicopter fly up in the air.
The main rotor collective pitch control i.e. (θ_0)angles all blades equally and simultaneously and allows the rotorcraft to raise vertically upward shown in Fig 2(a). The altitude of a helicopter is adjusted through collective pitch control, by changing blades pitch simultaneously. The longitudinal cyclic pitch angle (θ_{1s}) is between the rotor disk and airspeed caused by tilting the rotor disk either up (positive) or down (negative) shown in Fig 2(b). It allows the rotorcraft to move forward or backward.

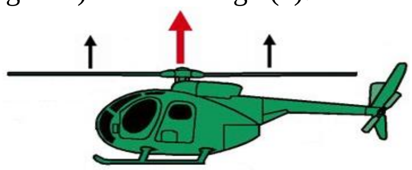

Fig 2(a): Main rotor collective pitch control

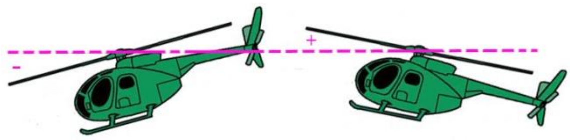

Fig 2(b): longitudinal cyclic pitch

Cyclic pitch control(θ_{1c}) allows each blade to be angled individually and allows the rotorcraft to move forward or backward, nose upward or downward, shown in Fig 2(c). The tail rotor collective pitch control (θ_{0T}) is used to counteract the torque effect shown in Fig 2(d). Yaw motion is performed by changing angle of attack of the tail rotor. Changing the pitch of the tail rotor blades will produce a side force that turns the rotorcraft nose left or right. During flight condition a pilot make changes to these four control inputs accordingly 6DOF motion of a rotorcraft is achieved.

Fig 2(c): Lateral cyclic pitch control

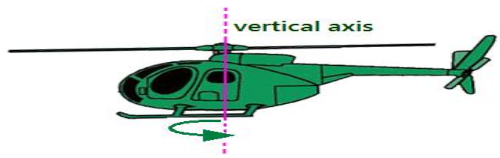

Fig 2(d): Tail rotor collective pitch

2. Nonlinear Equations of Motion

In nonlinear form the rotorcraft equation of motion can be written as:

$$\dot{x} = F(x, u, t) \quad (1)$$

Where "x" represents states and "u" represents four control inputs of a rotorcraft. States of the system are defined as;

$$x = [u, w, q, \theta, v, p, \varphi, r, \Psi] \quad (2)$$

Fig (3) shows different motion states of a rotorcraft i.e. roll, pitch & yaw.

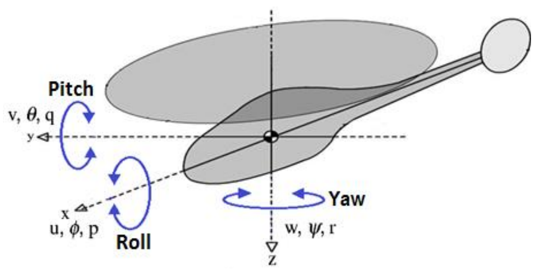

Fig 3: Different states of rotorcraft

Where (u, v, w)are translational velocities along x, y, z axis of helicopter body fixed frame; (p, q, r) are angular velocities about x-, y- and z-axes and (θ, Φ, Ψ) are Euler angles, defining position of body axes relative to the earth. Following are the 6 DOF nonlinear equations derived for a rotorcraft system.

$$\dot{u} = (rv - qw) + \frac{X}{M_a} - g\, sin\theta \tag{3}$$

$$\dot{v} = (pw - ru) + \frac{Y}{M_a} - g\, sin\Phi \tag{4}$$

$$\dot{w} = (qu - pv) + \frac{Z}{M_a} - g\, cos\Phi\, cos\theta \tag{5}$$

$$\dot{p} = \left(\frac{I_{yy}-I_{zz}}{I_{xx}}\right) qr + \frac{I_{xz}}{I_{xx}}(r + p\dot{q}) + L \tag{6}$$

$$\dot{q} = \left(\frac{I_{zz}-I_{xx}}{I_{yy}}\right) rp + \frac{I_{xz}}{I_{yy}}(r^2 - p^2) + M \tag{7}$$

$$\dot{r} = \left(\frac{I_{xx}-I_{yy}}{I_{zz}}\right) pq - \frac{I_{xz}}{I_{zz}}(p - qr) + N \tag{8}$$

$$\dot{\Phi} = p + tan\theta[qsin\Phi + rcos\Phi] \tag{9}$$

$$\dot{\theta} = qcos\Phi - rsin\Phi \tag{10}$$

$$\dot{\Psi} = [qsin\Phi + rcos\Phi]sec\theta \tag{11}$$

Using small perturbation theory the 6DOF nonlinear equations of motion are linearized given below to obtain the system state and control matrices. Detail procedure of linearization process of some nonlinear equations is given below;

2.1. Linearization of translational velocity

$$\dot{v} = (pw - ru) + \frac{Y}{M_a} - gsin\varphi cos\theta$$

Normalizing $\frac{1}{\mathrm{M_a}}$ i.e. mass of the helicopter,

$$\begin{aligned}\dot{v} = {} & (P_e + \Delta p)(W_e + \Delta w) - (R_e + \Delta r)(U_e + \Delta u) + Y_e + Y_u\Delta u + Y_w\Delta w + Y_q\Delta q + Y_\theta\Delta\theta + Y\Delta v + Y_p\Delta p \\ & + Y_\varphi\Delta\varphi + Y_r\Delta r + Y_{\theta_0}\Delta\theta_0 + Y_{\theta_{1s}}\Delta\theta_{1s} + Y_{\theta_{1c}}\Delta\theta_{1c} + Y_{\theta_{0T}}\Delta\theta_{0T} - gsin\varphi_e sin\theta_e\Delta\theta \\ & + gcos\varphi_e cos\theta_e\Delta\varphi\end{aligned}$$

Rearranging,

$$\begin{aligned}\dot{v} = {} & Y_u\Delta u - R_e\Delta u + Y_w\Delta w + P_e\Delta w + Y_q\Delta q - gsin\varphi_e sin\theta_e\Delta\theta + Y_v\Delta v + Y_p\Delta p + W_e\Delta p \\ & + gcos\varphi_e cos\theta_e\Delta\varphi + Y_r\Delta r - U_e\Delta r + Y_{\theta_0}\Delta\theta_0 + Y_{\theta_{1s}}\Delta\theta_{1s} + Y_{\theta_{1c}}\Delta\theta_{1c} + Y_{\theta_{0T}}\Delta\theta_{0T}\end{aligned}$$

$$\begin{aligned}\dot{v} = {} & \left(\frac{Y_u - R_e}{M_a}\right)\Delta u + \left(\frac{Y_w + P_e}{M_a}\right)\Delta w + \left(\frac{Y_q}{M_a}\right)\Delta q - gsin\varphi_e sin\theta_e\Delta\theta + \left(\frac{Y_v}{M_a}\right)\Delta v + \left(\frac{Y_p + W_e}{M_a}\right)\Delta p \\ & + gcos\varphi_e cos\theta_e\Delta\varphi + \left(\frac{Y_r + U_e}{M_a}\right)\Delta r + \left(\frac{Y_{\theta_0}}{M_a}\right)\Delta\theta_0 + \left(\frac{Y_{\theta_{1s}}}{M_a}\right)\Delta\theta_{1s} + \left(\frac{Y_{\theta_{1c}}}{M_a}\right)\Delta\theta_{1c} + \left(\frac{Y_{\theta_{0T}}}{M_a}\right)\Delta\theta_{0T}\end{aligned}$$

2.2. Linearization of Angular Velocity

$$I_{yy}\dot{q} = (I_{zz} - I_{xx})rp + I_{xz}(r^2 - p^2) + M$$

$$\dot{q} = \left(\frac{I_{zz}-I_{xx}}{I_{yy}}\right) rp + \left(\frac{I_{xz}}{I_{yy}}\right)(r^2 - p^2) + \frac{1}{I_{yy}}M$$

$$\dot{q} = \left(\frac{I_{zz}-I_{xx}}{I_{yy}}\right)(R_e\Delta p + P_e\Delta r) + \left(\frac{I_{xz}}{I_{yy}}\right)(2R_e\Delta r - 2P_e\Delta p) + (M_u\Delta u + M_w\Delta w + M_q\Delta q + M_\theta\Delta\theta + M_v\Delta v + M_p\Delta p + M_\varphi\Delta\varphi + M_r\Delta r + M_{\theta_0}\Delta\theta_0 + M_{\theta_{1s}}\Delta\theta_{1s} + M_{\theta_{1c}}\Delta\theta_{1c} + M_{\theta_{0T}}\Delta\theta_{0T})$$

$$\dot{q} = M_u\Delta u + M_w\Delta w + M_q\Delta q + M_v\Delta v + \left(M_p - 2P_e\frac{I_{xz}}{I_{yy}} + R_e\frac{I_{zz}-I_{xx}}{I_{yy}}\right)\Delta p + \left(M_r + 2R_e\frac{I_{xz}}{I_{yy}} + P_e\frac{I_{zz}-I_{xx}}{I_{yy}}\right)\Delta r + M_{\theta_0}\Delta\theta_0 + M_{\theta_{1s}}\Delta\theta_{1s} + M_{\theta_{1c}}\Delta\theta_{1c} + M_{\theta_{0T}}\Delta\theta_{0T}$$

2.3. Linearization of Euler Angles

$$\dot{\varphi} = p + qsin\varphi tan\theta + rcos\varphi tan\theta$$

$$\dot{\varphi} = \Delta p + sin\varphi_e tan\theta_e\Delta q + Q_e cos\varphi_e tan\theta_e\Delta\varphi + Q_e sin\varphi_e sec\theta_e\Delta\theta + cos\varphi_e tan\theta_e\Delta r - R_e sin\varphi_e tan\theta_e\Delta\varphi + R_e cos\varphi_e sec\theta_e\Delta\theta$$

$$\dot{\varphi} = (sin\varphi_e tan\theta_e)\Delta q + (Q_e sin\varphi_e sec\theta_e + R_e cos\varphi_e sec\theta_e)\Delta\theta + \Delta p + (Q_e cos\varphi_e tan\theta_e + R_e sin\varphi_e tan\theta_e)\Delta\varphi + (cos\varphi_e tan\theta_e)\Delta r$$

Now the linearized form of 6 DOF equations in state space is given by;

$$\dot{x} = Ax + Bu \qquad (12)$$

After linearizing the nonlinear equations of motion the system state and control matrices are obtained given in appendix (A) & (B).

3. Rotorcraft Model

In order to simulate the 6 DOF linearized equations of motion on a practical platform, stability derivatives data from Puma, SA330 helicopter has been used given in appendix (C). The dimensions of SA 330 Puma are given in Fig (4).

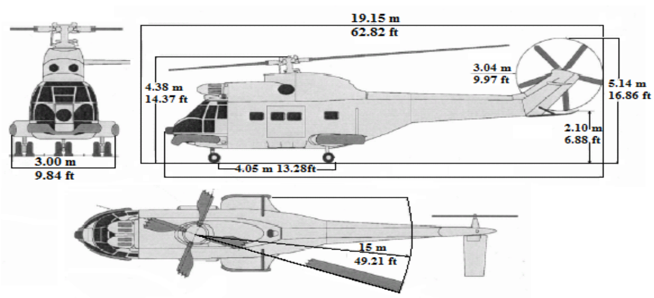

Fig 4: Puma, SA330, helicopter

4. Simulation Results

By applying 1 degree collective pitch to the rotor craft the response of the system is shown in Fig (5).

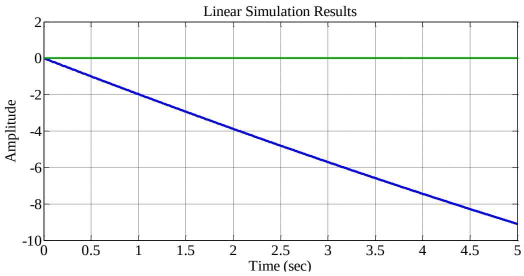

Eigenvalue	Damping	Freq. (rad/s)
2.02e-004 + 2.70e+001i	-7.49e-006	2.70e+001
2.02e-004 - 2.70e+001i	-7.49e-006	2.70e+001
-6.93e-001	1.00e+000	6.93e-001
-1.22e-001	1.00e+000	1.22e-001
-6.44e-002	1.00e+000	6.44e-002
-6.99e-004 + 1.25e-003i	4.88e-001	1.43e-003
-6.99e-004 - 1.25e-003i	4.88e-001	1.43e-003
7.14e-004	-1.00e+000	7.14e-004

Fig 5: Simulation results for 1 degree collective pitch

The plot indicates instability of the system. Instability is evident from eigenvalues of state matrix (A). The instability of the system can be better judged by the eigenvalues having positive real parts. To make the system stable an optimal controller is designed programmatically through Matlab/Simulink.
The block diagram of the feedback controller is given in Fig (6).

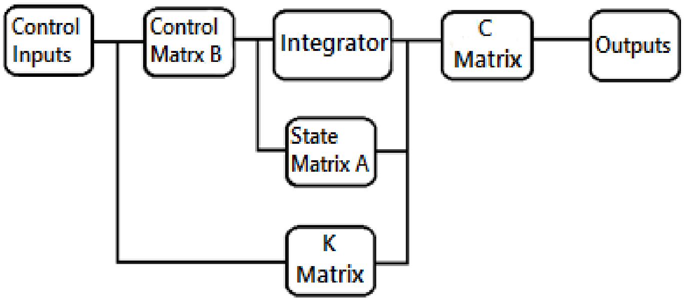

Fig 6: Block diagram of feedback controller

The closed loop stability is given by;

	Eigenvalue	Damping	Freq.(rad/s)
damp(A-B*K)	-1.60e+003	1.00e+000	1.60e+003
	-1.33e+002	1.00e+000	1.33e+002
	-1.47e+002	1.00e+000	1.47e+002
	-3.86e-001 + 2.72e+001i	1.42e-002	2.72e+001
	-3.86e-001 - 2.72e+001i	1.42e-002	2.72e+001
	-1.53e+000	1.00e+000	1.53e+000
	-6.82e-003	1.00e+000	6.82e-003
	-1.69e-004	1.00e+000	1.69e-004

The negative values show that the system is stable. In order to obtain a relationship between the maximum vertical speed (ω_s) and the collective pitch angle (θ_0) a transfer function is obtained;

$$\frac{\omega(s)}{\theta_0(s)} = \frac{-9775s^7 - 2.204e5s^6 - 8.477e6s^5 - 1.597e8s^4 - 9.271e8s^3 - 5.137e8s^2 - 2.943e6s - 4494}{s^8 + 144.7s^7 + 3598s^6 + 1.219e5s^5 + 2.072e6s^4 + 1.144e7s^3 + 6.327e6s^2 + 3.626e4s + 55.36}$$

Now applying 5 degree collective pitch the simulation results are given in Fig (7).

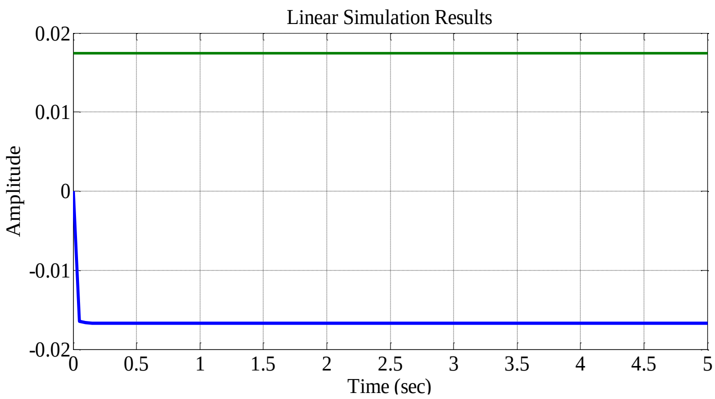

Fig 7: Simulation results for 5 degree collective pitch

The output of the model for different control inputs was observed the simulation results are shown in Fig (8).

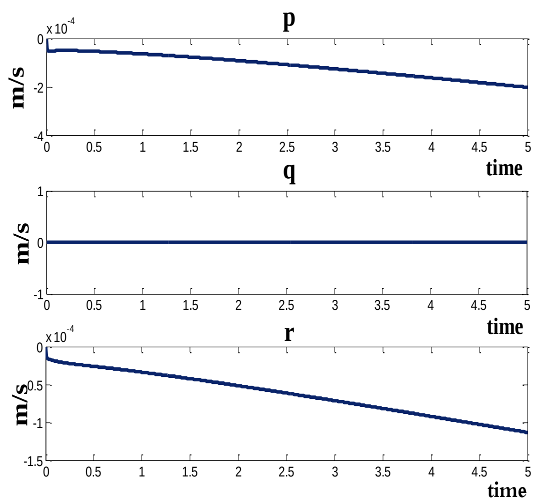

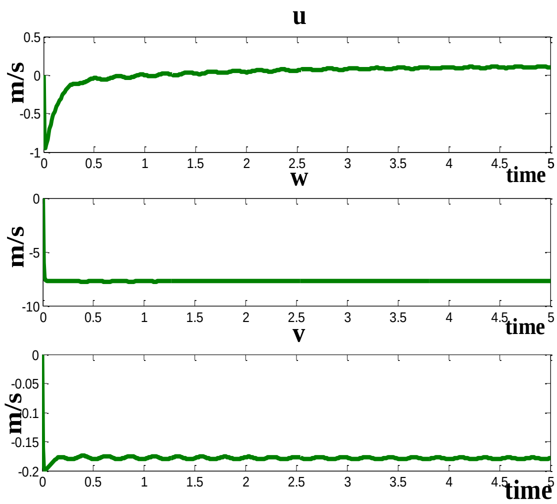

Fig 8: Rotational velocity components **Fig 9: Translational velocity components**

The plot shows angular velocities (p, q, and r) for a collective pitch of 5 degree and longitudinal cyclic pitch of 1.5 degree. Maximum hover rate is obtained i.e. 1500 ft/min. The collective pitch along with the longitudinal pitch is varied in order to reduce forward speed coupling. For above input control values plots of translational velocity (u, v, w) are show in Fig (9).

Similarly plots of Euler angles are shown in Fig (10).

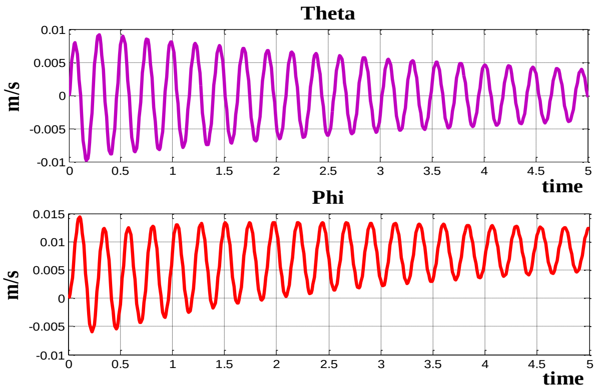

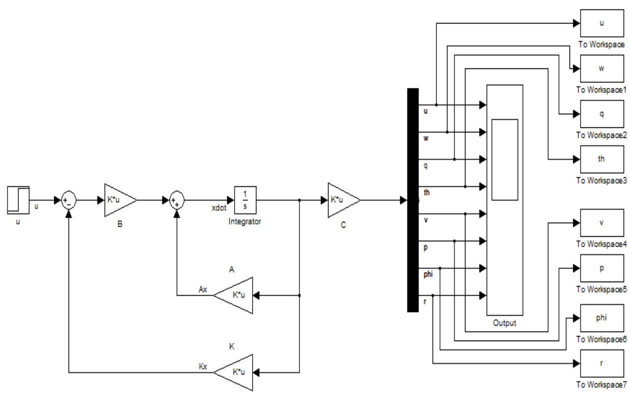

Fig 10: Euler Angles **Fig 11: Closed loop feedback controller**

The Closed loop feedback diagram which was developed using Simulink is given in Fig (11).

The C and K matrices has a great role in the performance of forward flight, for a forward flight, C matrix is changed by multiplying it with weighing factor (85). The C matrix becomes as such;

$$C = \begin{matrix} 85 & 0 & 0 & 0 & 0 & 0 & 0 & 0 \\ 0 & 85 & 0 & 0 & 0 & 0 & 0 & 0 \\ 0 & 0 & 85 & 0 & 0 & 0 & 0 & 0 \\ 0 & 0 & 0 & 85 & 0 & 0 & 0 & 0 \\ 0 & 0 & 0 & 0 & 85 & 0 & 0 & 0 \\ 0 & 0 & 0 & 0 & 0 & 85 & 0 & 0 \\ 0 & 0 & 0 & 0 & 0 & 0 & 85 & 0 \\ 0 & 0 & 0 & 0 & 0 & 0 & 0 & 85 \end{matrix}$$

The C and K matrices are modified to achieve best turn rates and speed outputs. Evaluation of better helicopter flight performance is achieved depending on the amount of available data about the helicopter.

5. Conclusion

In this paper we have studied the process of how to simulate the motion of blades considering four control inputs of a rotorcraft. The process comprised of linearization of 6DOF nonlinear equations of motion using small perturbation theory. Secondly the linearized model was used to obtain the state and control matrices for the stability of the rotorcraft. For simulation purpose input data of Puma SA330, helicopter was used. The final results were simulated for different values of control inputs using MATLAB/ Simulink program. LQR optimal controller is designed for the problem. However Linear Parameter Varying controller (LPV) or nonlinear controller can be implemented for better results. Another approach very popular these days are augmented controller using soft controlling techniques for aerial applications.

Appendices

(A) State matrix

$$A = \begin{bmatrix} X_u & X_w - Q_e & X_q - W_e & -g\cos\Theta_e & X_v + R_e & X_p & 0 & X_r - V_e \\ Z_u - Q_e & Z_w & Z_q + U_e & -g\cos\Phi_e\sin\Theta_e & Z_v - P_e & Z_p - V_e & -g\sin\Phi_e\sin\Theta_e & Z_r \\ M_u & M_w & M_q & 0 & M_v & \begin{matrix} M_p + 2P_e I_{xz}/I_{yy} \\ -R_e(I_{xx} - I_{zz})/I_{yy} \end{matrix} & 0 & \begin{matrix} M_r + 2R_e I_{xz}/I_{yy} \\ -P_e(I_{xx} - I_{zz})/I_{yy} \end{matrix} \\ 0 & 0 & \cos\Phi_e & 0 & 0 & 0 & -\Omega_a\cos\Theta_e & -\sin\Phi_e \\ Y_u - R_e & Y_w + P_e & Y_q & -g\sin\Phi_e\sin\Theta_e & Y_v & Y_p + W_e & g\cos\Phi_e\cos\Theta_e & Y_r - U_e \\ L_u' & L_w' & L_q' - k_1 P_e - k_2 R_e & 0 & L_v' & L_p' - k_1 Q_e & 0 & L_r' - k_2 Q_e \\ 0 & 0 & \sin\Phi_e\tan\Theta_e & \Omega_a\sec\Theta_e & 0 & 1 & 0 & \cos\Phi_e\tan\Theta_e \\ N_u' & N_w' & N_q' - k_1 R_e - k_3 P_e & 0 & N_v' & N_p' - k_3 Q_e & 0 & N_r' - k_1 Q_e \end{bmatrix}$$

(B) Control matrix

$$B = \begin{bmatrix} X_{\theta_0} & X_{\theta_{1s}} & X_{\theta_{1c}} & X_{\theta_{0T}} \\ Z_{\theta_0} & Z_{\theta_{1s}} & Z_{\theta_{1c}} & Z_{\theta_{0T}} \\ M_{\theta_0} & M_{\theta_{1s}} & M_{\theta_{1c}} & M_{\theta_{0T}} \\ 0 & 0 & 0 & 0 \\ Y_{\theta_0} & Y_{\theta_{1s}} & Y_{\theta_{1c}} & Y_{\theta_{0T}} \\ L'_{\theta_0} & L'_{\theta_{1s}} & L'_{\theta_{1c}} & L'_{\theta_{0T}} \\ 0 & 0 & 0 & 0 \\ N'_{\theta_0} & N'_{\theta_{1s}} & N'_{\theta_{1c}} & N'_{\theta_{0T}} \end{bmatrix}$$

where: $X_i = X_i / M_a,\; Y_i = Y_i / M_a,\; Z_i = Z_i / M_a$

$$L_i' = \frac{I_{zz}}{I_{xx}I_{zz} - I_{xz}^2} L_i + \frac{I_{xz}}{I_{xx}I_{zz} - I_{xz}^2} N_i \qquad k_1 = \frac{I_{xz}(I_{zz} + I_{xx} - I_{yy})}{I_{xx}I_{zz} - I_{xz}^2}$$

$$N_i' = \frac{I_{xz}}{I_{xx}I_{zz} - I_{xz}^2} L_i + \frac{I_{xx}}{I_{xx}I_{zz} - I_{xz}^2} N_i \qquad k_2 = \frac{I_{zz}(I_{zz} - I_{yy}) + I_{xz}^2}{I_{xx}I_{zz} - I_{xz}^2}$$

$$\Omega_a = \dot{\Psi} \quad (\textit{turn rate}) \qquad k_3 = \frac{I_{xx}(I_{yy} - I_{xx}) + I_{xz}^2}{I_{xx}I_{zz} - I_{xz}^2}$$

(C) Stability derivates data from wind tunnel for Puma SA330, helicopter.

$X_u = -0.0275\ 1/s$	$Z_u = -0.026\ 1/s$	$M_u = 0.03\ rad/s.m$	$X_{\theta_0} = -2.5\ m/s^2 rad$	$L_{\theta_0} = -7.5\ 1/s^2$	$I_{xx} = 9638\ kg.m^2$
$X_v = 0.006\ 1/s$	$Z_v = 0.03\ 1/s$	$M_v = -0.004\ rad/s.m$	$X_{\theta_{1S}} = -9.4\ m/s^2 rad$	$L_{\theta_{1S}} = -3\ 1/s^2$	$I_{xz} = 2226\ kg.m^2$
$X_w = 0.004\ 1/s$	$Z_w = 0.004\ 1/s$	$M_w = -0.025\ rad/s.m$	$X_{\theta_{1C}} = 0.5\ m/s^2 rad$	$L_{\theta_{1C}} = 25\ 1/s^2$	$I_{yy} = 33{,}240\ kg.m^2$
$X_p = 0.33\ m/s.rad$	$Z_p = 0.85\ m/s.rad$	$M_p = -0.22\ 1/s$	$X_{\theta_{0T}} = 0$	$L_{\theta_{0T}} = 5.3\ 1/s^2$	$I_{zz} = 25{,}889\ kg.m^2$
$X_q = 1.5\ m/s.rad$	$Z_q = 1.5\ m/s.rad$	$M_q = -0.75\ 1/s$	$Y_{\theta_0} = -3.2\ m/s^2 rad$	$M_{\theta_0} = 2.5\ 1/s^2$	$\Omega_a = 27\ rad/s$
$X_r = 0$	$Z_r = 0$	$M_r = 0$	$Y_{\theta_{1S}} = -0.7\ m/s^2 rad$	$M_{\theta_{1S}} = 7.5\ 1/s^2$	
$Y_u = -0.005\ 1/s$	$L_u = -0.005\ rad/s.m$	$N_u = 0.008\ rad/s.m$	$Y_{\theta_{1C}} = 10\ m/s^2 rad$	$M_{\theta_{1C}} = 0$	
$Y_v = -0.133\ 1/s$	$L_v = -0.045\ rad/s.m$	$N_v = 0.02\ rad/s.m$	$Y_{\theta_{0T}} = 5\ m/s^2 rad$	$M_{\theta_{0T}} = 0$	
$Y_w = 0.0225\ 1/s$	$L_w = -0.055\ rad/s.m$	$N_w = 0.035\ rad/s.m$	$Z_{\theta_0} = -115\ m/s^2 rad$	$N_{\theta_0} = -5\ 1/s^2$	
$Y_p = -1.5\ m/s.rad$	$L_p = -1.66\ 1/s$	$N_p = 0$	$Z_{\theta_{1S}} = -41\ m/s^2 rad$	$N_{\theta_{1S}} = 1.67\ 1/s^2$	
$Y_q = 0.33\ m/s.rad$	$L_q = 1\ 1/s$	$N_q = -0.25\ 1/s$	$Z_{\theta_{1C}} = 0$	$N_{\theta_{1C}} = 0$	
$Y_r = -52\ m/s.rad$	$L_r = -0.35\ 1/s$	$N_r = -0.625\ 1/s$	$Z_{\theta_{0T}} = 0$	$N_{\theta_{0T}} = -9.5\ 1/s^2$	

References

[1] Arcidiacono, P.J. (1969). “Prediction of Rotor Instability at High Forward Speeds”, Steady Flight Differential Equations of Motion for a Flexible Helicopter Blade with Chordwise Mass Unbalance, USAAVLABS, Vol. 1, TR 68-18A.

[2] Baraff, D. (1989). “Analytical methods for dynamic simulation of non-penetrating rigid bodies” In: SIGGRAPH ’89. pp. 223–232

[3] Datta, A. (2004). “Fundamental Understanding, Prediction and Validation of Rotor Vibratory Loads in Stedy Level Flight” Doctoral Thesis, University of Maryland, College Park, MD, USA.

[4] Houbolt, J.C., and Brooks, G.W. (1958). “Differential Equations of Motion for Combined Flap wise Bending, Chordwise Bending, and Torsion of Twisted, Nonuniform Rotor Blades” NACA Rep. 1346.

[5] Ilkko *et al.*., (2011). “Simulation of a helicopter rotor flow” *Rakenteiden Mekaniikka (Journal of Structural Mechanics)* Vol. 44, No. 3, 2, pp 186–205.

[6] Mil’, *et al.*, (1967). “Helicopters Calculation and Design” Aerodynamics, Vol. 1, NASA TT F-494.

[7] Potsdam *et al.*, (2006). “Rotor Airloads Prediction Using Loose Aerodynamically/Structural Coupling” *Journal of Aircraft*, Vol.43, No. 3, pp 732–742.

[8] Thanapalan, K.K.T. (2010). “Modeling of a Helicopter System” Faculty of Engineering Sciences University College London WC1E 6BT, U.K.

[9] Zioutis *et al.*, (2009). “Influence of Helicopter Rotor Wake Modeling on Blade Airload Predictions” *International Journal of Engineering (IJE)*, Vol. 3, Issue (6) 521.